A Probability Flux Approach for Binary Dynamics on Networks

Mohamad Riyadi[1], Agus Yodi Gunawan[2], and Dewi Handayani[2]

***Abstract*—Binary-state dynamics on networks provide a powerful framework for modeling epidemics and related spreading processes. Two main approaches are commonly used, namely exact continuous-time Markov chain (CTMC) formulations and mean-field approximations. The CTMC approach ensures stochastic accuracy but suffers from exponential state-space growth, whereas mean-field approximations lose reliability in heterogeneous or small networks. In this study, we formulate the master equation for binary dynamics using a probability flux approach, yielding an exact formulation for arbitrary networks. By integrating local transition rules, network topology, and state-space partitioning, the framework captures microscopic dynamics while enabling macroscopic analysis. Numerical simulations reveal that both state probabilities and expected infection levels are influenced not only by mean degree but also by structural heterogeneity. For instance, star and line topologies exhibit distinct behaviors despite having identical connectivity. Spectral analysis confirms the asymptotic stability of the disease-free equilibrium, while invariance under node relabeling emphasizes the role of graph symmetries in reducing state-space complexity. This work extends flux-based theory to network epidemics and provides a foundation for future studies on adaptive or time-varying networks.**

Index Terms - Binary dynamics, probability flux, master equation, CTMC, epidemic processes, network topology, structural heterogeneity.

I. INTRODUCTION

BINARY dynamics on networks are a central theme in network science. Numerous applications have been formulated in this framework, such as the susceptible/infected states in epidemic spreading [1], [2], [3], [4], the voter and q-voter models in opinion and social dynamics [5], [6], [7], [8], the Bass diffusion model for product adoption [10], contagion processes in social systems [11], [12], or quiescent–active–quiescent transitions in neuroscience [13]. These models provide a versatile framework for analyzing how local interactions generate macroscopic spreading phenomena in complex networks. Unlike well-mixed population models, network-based approaches account for topological heterogeneity, which has been shown to shape transmission rates and persistence patterns [3]. The explicit representation of nodes (e.g., individuals or locations) and edges (e.g., contacts or relations) further enables the analysis of graph-theoretic parameters—such as node degree—in examining how local interactions drive global dynamics [14], [15].

While exact formulations based on continuous-time Markov chains (CTMC) yield accurate stochastic descriptions, the exponential state-space size (2^N) renders them impractical for large networks. Conversely, approximate schemes such as mean-field and approximate master equations (AME) achieve scalability at the cost of microstate-level accuracy, particularly in small or heterogeneous graphs or when network symmetries play a critical role [16], [17], [18]. This methodological gap highlights the need for a formulation that remains exact, physically interpretable, and compatible with symmetry-based reductions.

Addressing this gap motivates the use of flux-based approaches, whose conceptual foundation was introduced by Schnakenberg [19] and later developed within stochastic thermodynamics to describe cycle currents, entropy production, and nonequilibrium phenomena [20], [21], [22]. In stochastic chemistry and systems biology, probability flux has been applied to study state flows, stochastic oscillations, and probability velocity fields [23], [24]. However, its application to binary dynamics on networks remains limited. Kiss et al. [4] derived master equations using flux-based illustrations, but only for the small case of $N = 3$, without providing a systematic generalization.

This paper introduces a probability flux formulation that is generic for arbitrary local transition rules, with explicit construction for $N = 3$ and systematic generalization to larger networks. Through numerical studies on diverse topologies (complete, line, star, lollipop, toast, cycle), we show how network structure influences probability distributions and the expected number of nodes in a given status, as exemplified in epidemic processes. In doing so, this work bridges exact stochastic accuracy with structural insight and extends the scope of flux-based theory to binary dynamics on networks.

The structure of this article is organized as follows. Section II reviews relevant literature on network and continuous-time Markov chains (CTMC), providing the theoretical foundation for binary dynamics. Section III introduces the probability flux approach to derive the master equation for binary dynamics on networks. Section IV presents the detailed formulation of the master equation, including an explicit derivation for the case $N = 3$. Section V presents numerical simulations of the Susceptible–Infected–Susceptible (SIS) model across different graph structures, illustrating the effects of network topology on the dynamics. Finally, Section VI concludes with a summary of the main findings and outlines potential directions for future research.

[1]M. Riyadi is with Doctoral Program in Mathematics, The Faculty of Mathematics and Natural Sciences, Institut Teknologi Bandung, Indonesia email:mhd.mriyadi@gmail.com

[2]A. Y. Gunawan is with Department of Mathematics, The Faculty of Mathematics and Natural Sciences, Institut Teknologi Bandung, Indonesia email: ayodi@itb.ac.id

[2]D. Handayani is with Department of Mathematics, The Faculty of Mathematics and Natural Sciences, Institut Teknologi Bandung, Indonesia email: dhandayanimtk@itb.ac.id

Manuscript received October 4, 2025; accepted November 5, 2025.

II. LITERATURE REVIEW

A. Network

Network structures provide a powerful framework for modeling interactions among discrete units in complex systems, including the spread of infectious diseases. In contrast to well-mixed population models, network-based approaches allow for explicit representation of heterogeneous contacts, which are critical for understanding the dynamics of contagion processes [4].

A network is mathematically defined as a graph $\mathcal{G} = (V, E)$, where $V = \{1, 2, \ldots, N\}$ is the set of nodes (e.g., individuals or cities) and $E \subseteq V \times V$ is the set of edges representing interactions. The structure of a graph can be encoded in an adjacency matrix $G = (g_{ij})_{i,j=1,\ldots,N}$, where $g_{ij} = 1$ if node i is connected to node j, and $g_{ij} = 0$ otherwise. For undirected simple graphs-used in this study-G is symmetric with zero diagonal entries, implying the absence of self-loops.

A fundamental characteristic influencing epidemic spread on networks is the *degree distribution*, which captures the heterogeneity in node connectivity. For node i, the degree is defined as:

$$k_i = \sum_{j=1}^{N} g_{ij},$$

and the average degree is given by:

$$\langle k \rangle = \frac{1}{N} \sum_{i=1}^{N} k_i = \frac{1}{N} \sum_{i=1}^{N} \sum_{j=1}^{N} g_{ij}.$$

B. CTMC

To describe the temporal evolution of states on such networks, we employ the framework of continuous-time Markov chains (CTMCs). Let $\mathcal{S}(t)$, a random variable, denote the system state at time t, taking values in the finite state space $\mathbf{S} = \{\mathcal{S}_1, \mathcal{S}_2, \ldots, \mathcal{S}_n\}$, where n is the number of states. The transition rate from state $\mathcal{S}_i$ to $\mathcal{S}_j$, for $i \neq j$, is denoted by $h(\mathcal{S}_i, \mathcal{S}_j)$. The diagonal elements are defined to ensure conservation of probability $h(\mathcal{S}_i, \mathcal{S}_i) = -\sum_{j \neq i} h(\mathcal{S}_i, \mathcal{S}_j)$, so that the total probability flux out of each state is zero $\sum_{j=1}^{n} h(\mathcal{S}_i, \mathcal{S}_j) = 0$. Letting $q_{ij} = h(\mathcal{S}_i, \mathcal{S}_j)$, we define the generator matrix $\mathbf{Q} = [q_{ij}] \in \mathbb{R}^{n \times n}$, where each row sums to zero and $q_{ij} \geq 0$ for $i \neq j$.

The transition probability over a small time interval δt satisfies

$$P(\mathcal{S}(t + \delta t) = \mathcal{S}_j \mid \mathcal{S}(t) = \mathcal{S}_i) = h(\mathcal{S}_i, \mathcal{S}_j)\delta t + o(\delta t),$$

where $o(\delta t)/\delta t \to 0$ as $\delta t \to 0$. Applying the law of total probability yields the master equation for the probability $X_j(t) = P(\mathcal{S}(t) = \mathcal{S}_j)$:

$$\frac{dX_j(t)}{dt} = \sum_{i=1}^{n} q_{ij} X_i(t).$$

In matrix form, this becomes

$$\dot{\mathbf{X}} = \mathbf{P}\mathbf{X}, \tag{1}$$

where $\mathbf{X} = (X_1, \ldots, X_n)^{\mathsf{T}}$ and $\mathbf{P}$ is the transpose of the rate matrix $\mathbf{Q}$, defined by $P_{ji} = q_{ij}$ for $j \neq i$ and $P_{jj} = -\sum_{k \neq j} q_{jk}$. Each column of $\mathbf{P}$ sums to zero, preserving the total probability mass.

III. MASTER EQUATION FOR BINARY DYNAMICS ON NETWORKS: A PROBABILITY FLUX APPROACH

In binary dynamics on networks, each node can be in one of two statuses, such as Q (quiescent) or T (transmitting) and change over time. Assuming a Markov process with exponentially distributed inter-event times and local transition rates that depend only on a node's status and the number of neighbors in each status, the system forms a CTMC on a finite state space of size 2^N. Under these assumptions, the master equation can be constructed [25]. Here, we formulate the master equation for binary dynamics on arbitrary graphs using a probability flux approach. This formulation adapts the general framework of [4], including the use of binary status notation Q and T, which can represent a wide range of spreading processes such as epidemics, information diffusion, or behavioral adoption in networks.

For a network with N nodes, there are 2^N possible states. The state space $\mathbf{S} = \{\mathcal{S}_1, \ldots, \mathcal{S}_{2^N}\}$ can be partitioned into $\{\boldsymbol{\mathcal{C}}^{(0)}, \boldsymbol{\mathcal{C}}^{(1)}, \ldots, \boldsymbol{\mathcal{C}}^{(N)}\}$, where $\boldsymbol{\mathcal{C}}^{(k)} = \{\mathcal{S}_1^{(k)}, \ldots, \mathcal{S}_{c_k}^{(k)}\}$ contains all states that have exactly k nodes in status T with $c_k = \binom{N}{k}$. From any $\mathcal{S}_j^{(k)} \in \boldsymbol{\mathcal{C}}^{(k)}$, transitions occur only to $\boldsymbol{\mathcal{C}}^{(k+1)}$ (exactly one node changes $Q \to T$) or to $\boldsymbol{\mathcal{C}}^{(k-1)}$ (exactly one node changes $T \to Q$), and vice versa, as illustrated in Figure 1. At the boundaries, $\boldsymbol{\mathcal{C}}^{(0)}$ transitions only to $\boldsymbol{\mathcal{C}}^{(1)}$ and $\boldsymbol{\mathcal{C}}^{(N)}$ only to $\boldsymbol{\mathcal{C}}^{(N-1)}$. The *transition rates* are determined by (i) the process mechanism—via the functions f_{QT} and f_{TQ}—and (ii) the network topology, represented by the adjacency matrix $G = (g_{ij})_{i,j=1,\ldots,N}$, which specifies, for each node, how many neighbors are in each status. If node l is Q in $\mathcal{S}_j^{(k)}$, the $Q \to T$ transition to a state in $\boldsymbol{\mathcal{C}}^{(k+1)}$ occurs at rate $f_{QT}\big(n_T(l, \mathcal{S}_j^{(k)})\big)$, where $n_T(l, \mathcal{S}_j^{(k)})$ denotes the number of T-neighbors of l in state $\mathcal{S}_j^{(k)}$. If node l is T, the $T \to Q$ transition to a state in $\boldsymbol{\mathcal{C}}^{(k-1)}$ occurs at rate $f_{TQ}\big(n_Q(l, \mathcal{S}_j^{(k)})\big)$, where $n_Q(l, \mathcal{S}_j^{(k)})$ is the number of Q-neighbors. For simplicity, f_{QT} and f_{TQ} may be taken to depend only on these neighbor counts, although more general dependencies are possible. The master equation is then constructed on this state space using these transition rates.

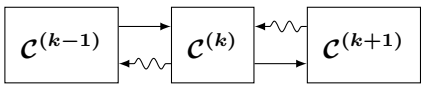

Fig. 1: Influx and outflux between classes of states

The dynamics over the state space can be modeled as a CTMC. Let $X_j^{(k)}(t)$ be the probability that the network is in state $\mathcal{S}_j^{(k)}$ at time t, for $j = 1, \ldots, c_k$. Define the vector

$$\mathbf{X}^{(k)}(t) = \left(X_1^{(k)}(t), X_2^{(k)}(t), \ldots, X_{c_k}^{(k)}(t)\right)^{\mathsf{T}},$$

which has dimension c_k for $k = 0, 1, \ldots, N$. The transitions described above lead to the master equation for each $X_j^{(k)}(t)$.

The master equation is derived using the concept of *probability flux*, which represents the rate of change in the probability of being in a specific state due to transitions to and from other states. Specifically, the probability flux from state $\mathcal{S}_j^{(k)} \in \boldsymbol{\mathcal{C}}^{(k)}$ to states in $\boldsymbol{\mathcal{C}}^{(k+1)}$ or $\boldsymbol{\mathcal{C}}^{(k-1)}$ is determined by the corresponding transition rate multiplied by $X_j^{(k)}(t)$.

For a given state $\mathcal{S}_j^{(k)}$, the total probability flux consists of:

Influx: Transitions from states in classes $(k-1)$ and $(k+1)$ to $\mathcal{S}_j^{(k)}$, which include

(i) Transitions from $\mathcal{S}_i^{(k-1)} \to \mathcal{S}_j^{(k)}$ occur when the two states differ at exactly one node l, which changes from Q to T. Each state in $\boldsymbol{\mathcal{C}}^{(k)}$ can be reached via up to k such transitions from $\boldsymbol{\mathcal{C}}^{(k-1)}$. The r-th transition rate is denoted $G_r^{(k-1)} = f_{QT}\big(n_T\big(l,\ \mathcal{S}_i^{(k-1)}\big)\big)$, with $r = 1, \ldots, k$. Here, $n_T\big(l,\ \mathcal{S}_i^{(k-1)}\big)$ is the number of neighbors of node l with status T in $\mathcal{S}_i^{(k-1)}$, computed as

$$n_T\big(l,\ \mathcal{S}_i^{(k-1)}\big) = \sum_{i \neq l}^{N} \delta_i\, g_{il},$$

where $\delta_i = 1$ if node i is in status T in $\mathcal{S}_i^{(k-1)}$, and $\delta_i = 0$ otherwise.

(ii) Transitions from $\mathcal{S}_i^{(k+1)} \to \mathcal{S}_j^{(k)}$ occur when the two states differ at exactly one node l, which changes from T to Q. Each state in $\boldsymbol{\mathcal{C}}^{(k)}$ can be reached via up to $N-k$ such transitions from $\boldsymbol{\mathcal{C}}^{(k+1)}$. The r-th transition rate is denoted $G_r^{(k+1)} = f_{TQ}\big(n_Q\big(l,\ \mathcal{S}_i^{(k+1)}\big)\big)$, with $r = 1, \ldots, N-k$, and $n_Q\big(l,\ \mathcal{S}_i^{(k+1)}\big)$ is the number of neighbors of node l with status Q in $\mathcal{S}_i^{(k+1)}$, calculated as

$$n_Q\big(l,\ \mathcal{S}_i^{(k+1)}\big) = \sum_{i \neq l}^{N} \delta_i\, g_{il},$$

with $\delta_i = 1$ if node i is in status Q in $\mathcal{S}_i^{(k+1)}$, and $\delta_i = 0$ otherwise.

Outflux: Transitions from $\mathcal{S}_j^{(k)}$ to states in classes $(k-1)$ and $(k+1)$, involving a change in the status of one node. Each such transition corresponds to

(i) A recovery at node l: transition $\mathcal{S}_j^{(k)} \to \mathcal{S}_i^{(k-1)}$, with rate $G_r^{(k^-)}$, for $r = 1, \ldots, k$.

(ii) An infection at node l: transition $\mathcal{S}_j^{(k)} \to \mathcal{S}_i^{(k+1)}$, with rate $G_r^{(k^+)}$, for $r = 1, \ldots, N-k$.

The time evolution of $X_j^{(k)}(t)$ consists of influx and outflux terms, yielding the master equation

$$\begin{aligned}\dot{X}_j^{(k)} = &\sum_{r=1}^{k} G_r^{(k-1)} X_r^{(k-1)} + \sum_{r=1}^{N-k} G_r^{(k+1)} X_r^{(k+1)} \\ &- \left(\sum_{r=1}^{N-k} G_r^{(k^-)} + \sum_{r=1}^{k} G_r^{(k^+)} \right) X_j^{(k)}, \\ &k = 0, 1, \ldots, N. \end{aligned} \tag{2}$$

Here, $X_r^{(k-1)}$ and $X_r^{(k+1)}$ represent the probabilities associated with incoming transitions to the state $\mathcal{S}_j^{(k)}$. Equation (2) defines a coupled system consisting of 2^N differential equations, corresponding to the full state space of the process. This system can be expressed in Equation (1), where $\mathbf{P}$ has a block tridiagonal structure. The tridiagonal nature of $\mathbf{P}$ reflects the fact that transitions only occur between neighboring classes $\boldsymbol{\mathcal{C}}^{(k-1)}$, $\boldsymbol{\mathcal{C}}^{(k)}$, and $\boldsymbol{\mathcal{C}}^{(k+1)}$. The structure of this block tridiagonal master equation has been described in detail in [15], [4], and [25].

IV. FORMULATION

We formulate the master equation for binary dynamics on arbitrary graphs. While Equation (2) applies to the case $N = 2$, we omit detailed discussion since it only yields a trivial line graph with limited exploratory value. For $N > 2$, more diverse graph structures can be formed—such as complete or line graphs—which allow for richer exploration. Each node in the graph can be in one of two binary statuses: Q or T. For $N = 3$, the total number of possible system states is $2^3 = 8$. For binary-state dynamics on a triangle graph, the Markov chain spans the state space

$$\mathbf{S} = \{QQQ, QQT, QTQ, TQQ, QTT, TQT, TTQ, TTT\}$$

with each element specifying the configuration of nodes 1–3. As an example, QQT corresponds to nodes 1 and 2 being in status Q, and node 3 in status T. We define the partition

$$\mathbf{S} = \{\boldsymbol{\mathcal{C}}^{(0)}, \boldsymbol{\mathcal{C}}^{(1)}, \boldsymbol{\mathcal{C}}^{(2)}, \boldsymbol{\mathcal{C}}^{(3)}\},$$

with

$$\begin{aligned}\boldsymbol{\mathcal{C}}^{(0)} &= \{QQQ\}, \\ \boldsymbol{\mathcal{C}}^{(1)} &= \{QQT, QTQ, TQQ\}, \\ \boldsymbol{\mathcal{C}}^{(2)} &= \{QTT, TQT, TTQ\}, \\ \boldsymbol{\mathcal{C}}^{(3)} &= \{TTT\},\end{aligned}$$

and c_k for $k = 0, 1, 2, 3$ equals 1, 3, 3, and 1, respectively.

The possible transitions between partition classes are shown in Figure 2, while all state configurations and their transitions are illustrated in Figure 3, where a transition occurs only if the two states differ by one node. At most one transition can occur at a time, although the interval between transitions can be arbitrarily small. For example, consider the state $QQT \in \boldsymbol{\mathcal{C}}^{(1)}$, as highlighted in Figure 3. Its possible transitions (influx and outflux) involve $\{QQQ\} \in \boldsymbol{\mathcal{C}}^{(0)}$ and $\{QTT, TQT\} \in \boldsymbol{\mathcal{C}}^{(2)}$.

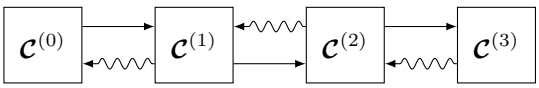

Fig. 2: Influx and outflux between the four partition classes $\boldsymbol{\mathcal{C}}^{(k)}$ for $k = 0, 1, 2, 3$.

In the transition from $\{QQQ\} \in \boldsymbol{\mathcal{C}}^{(0)}$ to $QQT \in \boldsymbol{\mathcal{C}}^{(1)}$, differing only at node 3, the transition rate is given by

$$\begin{aligned}G_1^{(1)} &= f_{QT}(n_T(i,3)) \\ &= f_{QT}\left(\sum_{i \neq l}^{3} \delta_i\, g_{i3} \right)\end{aligned}$$

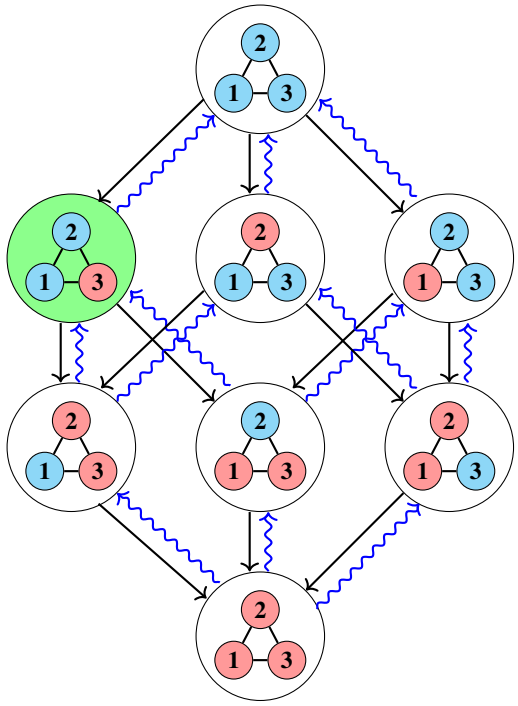

Fig. 3: Nodes in status Q (●) and T (●) are represented by color-coded filled circles.

$$= f_{QT}(\delta_1 g_{13} + \delta_2 g_{23})$$
$$= f_{QT}(0),$$

since $\delta_1 = \delta_2 = 0$, i.e., no nodes in status T in configuration QQQ. For transitions $\{QTT, TQT\} \in \boldsymbol{\mathcal{C}}^{(2)} \to QQT \in \boldsymbol{\mathcal{C}}^{(1)}$, which differ at node 2 and 1 respectively, the transition rates are:

$$G_1^{(2)} = f_{TQ}(\delta_1 g_{12} + \delta_3 g_{32}) = f_{TQ}(g_{12}),$$
$$G_2^{(2)} = f_{TQ}(\delta_2 g_{21} + \delta_3 g_{31}) = f_{TQ}(g_{21}),$$

where $\delta_1 = \delta_2 = 1$ since nodes 1 and 2 are in status Q in QTT and TQT, respectively, and $\delta_3 = 0$ because node 3 is in status T.

For the reverse (outflux) transitions from $\boldsymbol{\mathcal{C}}^{(1)}$ to $\boldsymbol{\mathcal{C}}^{(0)}$ and $\boldsymbol{\mathcal{C}}^{(2)}$, the rates are similarly computed as

$$\sum_{r=1}^{2} G_r^{(1^-)} = f_{QT}(g_{31}) + f_{QT}(g_{32}),$$
$$\sum_{r=1}^{1} G_r^{(1^+)} = f_{TQ}(g_{13} + g_{23}).$$

We denote X_{QQT} as the probability that the network is in state QQT. The probabilities corresponding to transitions from other states into QQT are X_{QQQ} as well as X_{QTT} and X_{TQT}. The evolution of X_{QQT}, and all other state probabilities, follows from the master equation. For a general graph with $N = 3$ nodes, the master equations are given as follows

$$\begin{aligned}
\dot{X}_{QQQ} &= f_{TQ}(g_{13} + g_{23}) X_{QQT} + f_{TQ}(g_{12} + g_{32}) X_{QTQ} \\
&\quad + f_{TQ}(g_{21} + g_{31}) X_{TQQ} - 3 f_{QT}(0) X_{QQQ} \\
\dot{X}_{QQT} &= f_{QT}(0) X_{QQQ} + f_{TQ}(g_{12}) X_{QTT} + f_{TQ}(g_{21}) X_{TQT} \\
&\quad - \left(f_{TQ}(g_{13} + g_{23}) + f_{QT}(g_{31}) + f_{QT}(g_{32})\right) X_{QQT} \\
\dot{X}_{QTQ} &= f_{QT}(0) X_{QQQ} + f_{TQ}(g_{13}) X_{QTT} + f_{TQ}(g_{31}) X_{TTQ} \\
&\quad - \left(f_{TQ}(g_{12} + g_{32}) + f_{QT}(g_{23}) + f_{QT}(g_{21})\right) X_{QTQ} \\
\dot{X}_{TQQ} &= f_{QT}(0) X_{QQQ} + f_{TQ}(g_{23}) X_{TQT} + f_{TQ}(g_{32}) X_{TTQ} \\
&\quad - \left(f_{TQ}(g_{21} + g_{31}) + f_{QT}(g_{12}) + f_{QT}(g_{13})\right) X_{TQQ} \\
\dot{X}_{QTT} &= f_{TQ}(0) X_{TTT} + f_{QT}(g_{32}) X_{QQT} + f_{QT}(g_{23}) X_{QTQ} \\
&\quad - \left(f_{TQ}(g_{12}) + f_{TQ}(g_{13}) + f_{QT}(g_{21} + g_{31})\right) X_{QTT} \\
\dot{X}_{TQT} &= f_{TQ}(0) X_{TTT} + f_{QT}(g_{31}) X_{QQT} + f_{QT}(g_{13}) X_{TQQ} \\
&\quad - \left(f_{TQ}(g_{21}) + f_{TQ}(g_{23}) + f_{QT}(g_{12} + g_{32})\right) X_{TQT} \\
\dot{X}_{TTQ} &= f_{TQ}(0) X_{TTT} + f_{QT}(g_{21}) X_{QTQ} + f_{QT}(g_{12}) X_{TQQ} \\
&\quad - \left(f_{TQ}(g_{31}) + f_{TQ}(g_{32}) + f_{QT}(g_{13} + g_{23})\right) X_{TTQ} \\
\dot{X}_{TTT} &= f_{QT}(g_{21} + g_{31}) X_{QTT} + f_{QT}(g_{12} + g_{32}) X_{TQT} \\
&\quad + f_{QT}(g_{13} + g_{23}) X_{TTQ} - 3 f_{TQ}(0) X_{TTT}
\end{aligned} \tag{3}$$

Equation (3) is identical to the master equation for binary dynamics on an arbitrary graph with $N = 3$ as presented in [4]. Similarly, the master equation for $N = 4$ can be derived.

V. SIS MODEL SIMULATION ACROSS GRAPH STRUCTURES

We conduct simulations of the model over several network structures for $N = 3$ and $N = 4$ nodes. The graph variations used in the simulation are illustrated in Figures 4 and 5. Without loss of generality, we focus our discussion on disease spread governed by the SIS dynamics on networks.

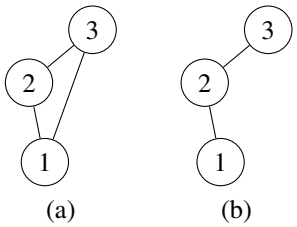

Fig. 4: (a) Complete graph; (b) Line graph with $N = 3$ nodes.

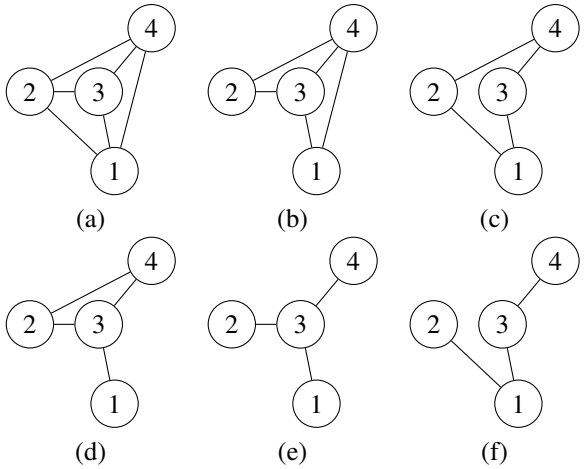

Fig. 5: Examples of $N = 4$ graph topologies: (a) complete, (b) toast, (c) cycle, (d) lollipop, (e) star, and (f) line graph.

In this model, each node exists in one of two possible states: susceptible (S) or infected (I), corresponding to the binary states $Q = S$ and $T = I$. The system evolves through two types of transitions: infection and recovery. The infection rate is defined as $f_{SI}(n) = \tau n$, where n is the number of infected neighbors and τ is the per-contact transmission rate. In contrast, the recovery rate is assumed constant and given by $f_{IS}(n) = \gamma$, independent of neighbor status.

Let X_{ABC} denote the probability that the network is in state ABC, where each letter represents the status of a node: S or I. The master equation for SIS dynamics on a complete graph with $N = 3$ nodes is derived as follows.

Consider, for instance, the state X_{SSI}. The infection and recovery rates are given by $f_{SI}(n) = \tau n$ and $f_{IS} = \gamma$, respectively. The adjacency matrix of the complete graph with $N = 3$

$$G = \begin{bmatrix} 0 & 1 & 1 \\ 1 & 0 & 1 \\ 1 & 1 & 0 \end{bmatrix}.$$

From Equation 3, the time evolution of X_{SSI} is given by:

$$\begin{aligned} \dot{X}_{SSI} &= f_{SI}(0)X_{SSS} + f_{IS}(g_{12})X_{SII} + f_{IS}(g_{21})X_{ISI} \\ &\quad - \left(f_{IS}(g_{13} + g_{23}) + f_{SI}(g_{31}) + f_{SI}(g_{32})\right) X_{SSI} \\ &= \gamma(X_{SII} + X_{ISI}) - (2\tau + \gamma)X_{SSI}, \end{aligned}$$

where we used $f_{SI}(0) = 0$ and substituted adjacency values from G. This procedure applies analogously to all other states, resulting in the full master equation for the system, namely

$$\begin{aligned} \dot{X}_{SSS} &= \gamma(X_{SSI} + X_{SIS} + X_{ISS}) \\ \dot{X}_{SSI} &= \gamma(X_{SII} + X_{ISI}) - (2\tau + \gamma)X_{SSI} \\ \dot{X}_{SIS} &= \gamma(X_{SII} + X_{IIS}) - (2\tau + \gamma)X_{SIS} \\ \dot{X}_{ISS} &= \gamma(X_{ISI} + X_{IIS}) - (2\tau + \gamma)X_{ISS} \\ \dot{X}_{SII} &= \gamma X_{III} + \tau(X_{SSI} + X_{SIS}) - 2(\tau + \gamma)X_{SII} \\ \dot{X}_{ISI} &= \gamma X_{III} + \tau(X_{SSI} + X_{ISS}) - 2(\tau + \gamma)X_{ISI} \\ \dot{X}_{IIS} &= \gamma X_{III} + \tau(X_{SIS} + X_{ISS}) - 2(\tau + \gamma)X_{IIS} \\ \dot{X}_{III} &= -3\gamma X_{III} + 2\tau(X_{SII} + X_{ISI} + X_{IIS}) \end{aligned} \tag{4}$$

For simulation, the initial condition assumes a single infected node with probability $1/N$. Since there are $\binom{N}{1}$ such states, the initial probability of each individual state in $\mathcal{C}^{(1)}$ is given by

$$\begin{aligned} \mathbf{X}(0) &= (0, 1/9, 1/9, 1/9, 0, 0, 0, 0)^{\mathsf{T}} \quad \text{for } N = 3, \\ \mathbf{X}(0) &= (0, 1/16, 1/16, 1/16, 1/16, 0, \ldots, 0)^{\mathsf{T}} \quad \text{for } N = 4. \end{aligned}$$

On a complete graph, all states with the same number of infected nodes are equivalent due to node symmetry (graph automorphism) [4]. For $N = 3$ and $N = 4$, the dynamics of states in the same class $\mathcal{C}^{(k)}$ are identical, as illustrated in Figure 6.

In the line graph with $N = 3$ (Figure 4b), symmetric states can be identified by reflection across the central node. For example, states SSI and ISS are equivalent, as are SII and IIS. Hence, the 2^3 state space can be regrouped as:

$$\mathcal{C}^{(0)} = \{SSS\},$$

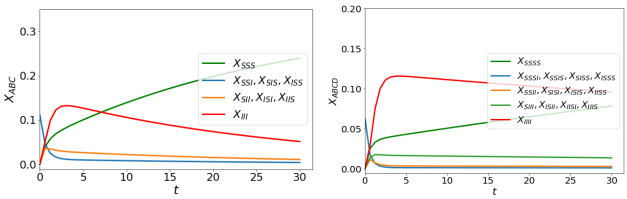

Fig. 6: Probabilities X_{ABC} and X_{ABCD} for the complete graph with $\tau = 0.7$ and $\gamma = 0.3$.

$$\begin{aligned} \mathcal{C}_1^{(1)} &= \{SSI, ISS\}, & \mathcal{C}_2^{(1)} &= \{SIS\}, \\ \mathcal{C}_1^{(2)} &= \{SII, IIS\}, & \mathcal{C}_2^{(2)} &= \{ISI\}, \\ \mathcal{C}^{(3)} &= \{III\}. \end{aligned}$$

The resulting dynamics for this topology are shown in Figure 7.

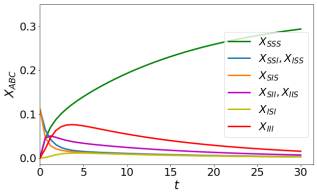

Fig. 7: State probabilities X_{ABC} for the line graph with 3 nodes; $\tau = 0.7$, $\gamma = 0.3$.

For the set of six graph structures with $N = 4$ nodes shown in Figure 5, the state probabilities are presented in Figure 8. Simulations indicate that the probability distribution over states is highly dependent on the connectivity of the underlying graph. Specifically, graphs with higher connectivity tend to have a greater probability mass concentrated in the fully infected state.

Numerical investigations show that in isomorphic graphs with identical node statuses, system dynamics remain invariant under node relabeling, even though the state representation changes. An illustrative example is given in Figure 9. Consider a line graph with $N = 3$ nodes labeled sequentially as 1–2–3, with the network state denoted by SSI and probability X_{SSI}. Suppose the node labels are permuted to form a new sequence 1–3–2, while the node-level statuses remain SSI. Under this relabeling, the state is mapped to SIS with corresponding probability Y_{SIS}, where the ordering of nodes is preserved from 1 to 3. Despite the relabeling, the time evolution of X_{SSI} is identical to that of Y_{SIS}. This invariance holds when transition rates are homogeneous and depend only on permutation-invariant neighborhood statistics, but it breaks down in the presence of node or edge heterogeneity, or other structural asymmetries.

Because system dynamics are invariant under node relabeling, analysis can focus on expectation values rather than individual trajectories. The expected number of infected nodes, $[I](t)$, is obtained as the weighted sum of infected nodes across all configurations [25]. This captures macroscopic outcomes without dependence on arbitrary labeling.

Numerical simulations show that network topology strongly influences infection prevalence. As illustrated in Figure 10,

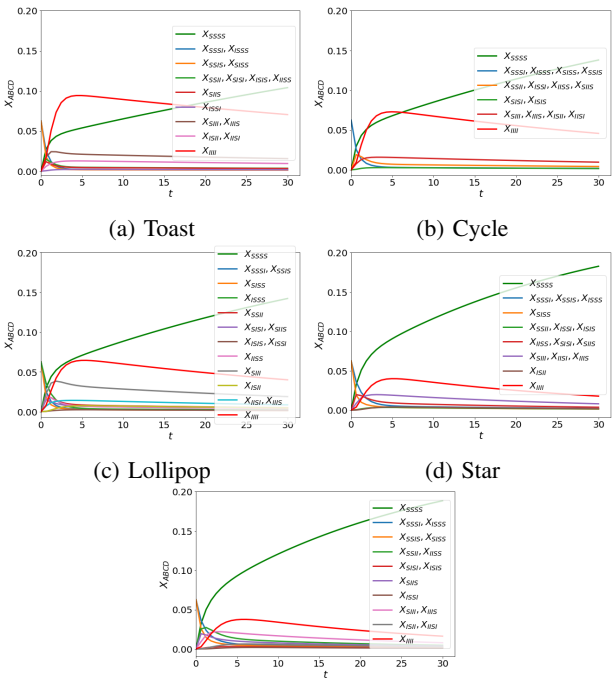

(a) Toast (b) Cycle

(c) Lollipop (d) Star

(e) Line

Fig. 8: State probabilities X_{ABCD} across graph topologies with $\tau = 0.7$, $\gamma = 0.3$.

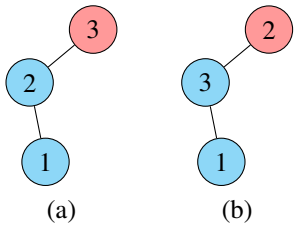

(a) (b)

Fig. 9: Invariance under node relabeling on isomorphic line graphs with $N = 3$ (● = susceptible, ● = infected). (a) Labeling 1–2–3 yield the state SSI and probability X_{SSI}. (b) Relabeling to 1–3–2 maps the same node-level configuration to SIS with probability Y_{SIS}.

denser graphs with higher average degree, such as the complete ($\langle k \rangle = 3$) and toast ($\langle k \rangle = 5/2$) graphs, sustain higher $[I](t)$. By contrast, sparse networks like line and star ($\langle k \rangle = 3/2$) exhibit lower prevalence due to limited transmission pathways. Circle and lollipop graphs ($\langle k \rangle = 2$) fall between these extremes, highlighting the combined role of degree distribution and structural features.

These findings indicate that both probabilities that the system in a given state and expected infection levels depends not only on average degree but also on structural heterogeneity. For instance, the star and line graphs share the same $\langle k \rangle$ yet differ in dynamics due to centralization and path length. This supports theoretical results that both average connectivity and network topology shape epidemic stability and persistence [3], [14].

Spectral analysis of the transition rate matrix is key to understanding the long-term behavior of SIS epidemiological

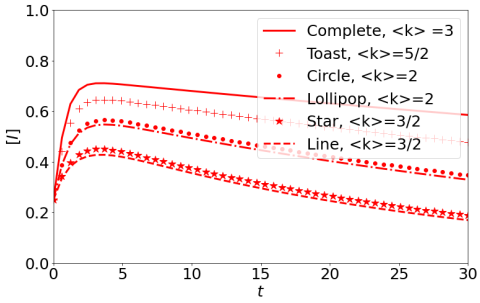

Fig. 10: Expected value $[I](t)$ across different network topologies ($N = 4$), highlighting the impact of average degree and structural heterogeneity.

systems. We consider the disease-free equilibrium, character-

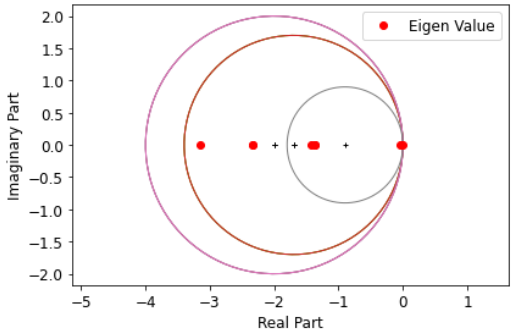

Fig. 11: Gershgorin disks (circles) and eigenvalues (red dots) of the transition rate matrix $\mathbf{P}$ for a continuous-time Markov chain modeling SIS dynamics on a complete graph with $N = 3$ nodes. All eigenvalues lie within the left half of the complex plane, confirming that the real parts are non-positive. This supports the conclusion that the system exhibits asymptotic stability or converges to an absorbing disease-free state.

ized by $\dot{\mathbf{X}} = 0$ in Equation (1). Since the first column of $\mathbf{P}$ consists entirely of zeros [25], the system has a steady-state solution $\mathbf{X}^* = \mathbf{e}_1$, representing the state in which all nodes are susceptible. To assess the stability of this equilibrium, we apply the Gershgorin Circle Theorem [15]. Applying this theorem to the column structure of $\mathbf{P}$, we find that all Gershgorin disks are centered on the negative real axis and lie entirely in the left half of the complex plane. This implies that all eigenvalues have non-positive real parts, $\mathrm{Re}(\lambda) \leq 0$, which guarantees that the system asymptotically approaches a stable or absorbing state. Figure 11 illustrates the spectral structure of the transition rate matrix $\mathbf{P}$ using Gershgorin disks and its eigenvalues.

VI. CONCLUSIONS

This study formulated the master equation for binary dynamics on arbitrary networks using a probability flux approach, providing an exact and interpretable alternative to mean-field approximations. By incorporating local transition rules, network topology, and state-space partitioning, the

method provided a description of spreading processes across diverse graph structures.

Numerical simulations showed that both state probabilities and expected infected nodes depend not only on average degree but also on structural heterogeneity, with topologies such as stars and lines exhibiting distinct dynamics despite identical mean connectivity. Spectral analysis confirmed that the disease-free equilibrium was asymptotically stable, as all eigenvalues of the transition rate matrix had non-positive real parts. Moreover, invariance under node relabeling highlighted the role of graph symmetries in reducing state-space complexity.

These findings extend flux-based theory to epidemic and binary-state dynamics on networks, with potential applications to modeling disease spread in urban contact networks and diffusion processes in social or technological systems. Future work warrants explore extensions to time-varying or adaptive networks, offering insights into resilience and control strategies in dynamic environments.

ACKNOWLEDGMENT

The authors gratefully acknowledge the support from the Ministry of Education, Culture, Research, and Technology of the Republic of Indonesia (Kemendikbud Ristek) through the Doctoral Dissertation Research Grant (PDD) scheme in 2024 under Contract No.: 223/IT1.B07.1/SPP-LPPM/VI/2024.

REFERENCES

[1] R. M. Anderson and R. M. May, *Infectious Diseases of Humans: Dynamics and Control*, vol. 1, Oxford University Press, Oxford, 1991.
[2] R. Pastor-Satorras and A. Vespignani, "Epidemic spreading in scale-free networks," *Physical Review Letters*, vol. 86, no. 14, p. 3200, 2001.
[3] R. Pastor-Satorras, C. Castellano, P. Van Mieghem, and A. Vespignani, "Epidemic processes in complex networks," *Reviews of Modern Physics*, vol. 87, no. 3, pp. 925–979, 2015.
[4] I. Z. Kiss, J. C. Miller, and P. L. Simon, *Mathematics of Epidemics on Networks: From Exact to Approximate Models*. Cham: Springer, 2017.
[5] V. Sood and S. Redner, "Voter model on heterogeneous graphs," *Physical Review Letters*, vol. 94, no. 17, p. 178701, 2005.
[6] C. Castellano, D. Vilone, and A. Vespignani, "Incomplete ordering of the voter model on small-world networks," *Europhysics Letters*, vol. 63, no. 1, pp. 153–158, 2003.
[7] C. Castellano, M. A. Muñoz, and R. Pastor-Satorras, "Nonlinear q-voter model," *Physical Review E*, vol. 80, no. 4, p. 041129, 2009.
[8] F. Vazquez and V. M. Eguíluz, "Analytical solution of the voter model on uncorrelated networks," *New Journal of Physics*, vol. 10, no. 6, p. 063011, 2008.
[9] J. A. Ward and M. López-García, "Exact analysis of summary statistics for continuous-time discrete-state Markov processes on networks using graph-automorphism lumping," *Applied Network Science*, vol. 4, p. 108, 2019. DOI: 10.1007/s41109-019-0206-4.
[10] F. M. Bass, "A new product growth for model consumer durables," *Management Science*, vol. 15, no. 5, pp. 215–227, 1969.
[11] A. L. Hill, D. G. Rand, M. A. Nowak, and N. A. Christakis, "Infectious disease modeling of social contagion in networks," *PLoS Computational Biology*, vol. 6, no. 11, p. 1000968, 2010.
[12] D. J. Watts, "A simple model of global cascades on random networks," *Proceedings of the National Academy of Sciences*, vol. 99, no. 9, pp. 5766–5771, 2002.
[13] J. D. Cowan, "Stochastic Neurodynamics," in *Proceedings of the 1990 Conference on Advances in Neural Information Processing Systems 3*, Morgan Kaufmann Publishers Inc., San Francisco, CA, 1990.
[14] P. Van Mieghem, "The N-intertwined SIS epidemic network model," *Computing*, vol. 93, no. 2–4, pp. 147–169, 2011.
[15] P. Van Mieghem, J. Omic, and R. Kooij, "Virus spread in networks," *IEEE/ACM Transactions on Networking*, vol. 17, no. 1, pp. 1–14, 2008.
[16] I. Z. Kiss, J. C. Miller, and P. L. Simon, "Approximate master equations for dynamical processes on graphs," *Mathematical Modelling of Natural Phenomena*, vol. 9, no. 2, pp. 43–57, 2014.
[17] J. P. Gleeson, "High-accuracy approximation of binary-state dynamics on networks," *Physical Review Letters*, vol. 107, no. 6, 068701, 2011.
[18] G. St-Onge, J.-G. Young, L. Hébert-Dufresne, L. J. Dubé, and P. Desrosiers, "Master equation analysis of non-Markovian dynamics on networks," *Physical Review E*, vol. 103, no. 3, 032301, 2021.
[19] J. Schnakenberg, "Network theory of microscopic and macroscopic behavior of master equation systems," *Reviews of Modern Physics*, vol. 48, no. 4, pp. 571–585, 1976.
[20] M. Esposito and C. Van den Broeck, "Three faces of the second law. I. Master equation formulation," *Physical Review E*, vol. 82, 011143, 2010.
[21] T. Tomé and M. J. de Oliveira, "Stochastic thermodynamics and entropy production of chemical reaction systems," *The Journal of Chemical Physics*, vol. 148, no. 22, 224104, 2018.
[22] M. F. Weber and E. Frey, "Master equations and the theory of stochastic path integrals," *Reports on Progress in Physics*, vol. 80, no. 4, 046601, 2017.
[23] Y. Cao, A. Terebus, and J. Liang, "Accurate chemical master equation solution using multi-finite buffers," *Multiscale Modeling & Simulation*, vol. 14, no. 2, pp. 923–963, 2016.
[24] A. Terebus, C. Liu, and J. Liang, "Discrete flux and velocity fields of probability and their global maps in reaction systems," *The Journal of Chemical Physics*, vol. 149, no. 18, 185101, 2018.
[25] P. L. Simon, M. Taylor, and I. Z. Kiss, "Exact epidemic models on graphs using graph-automorphism driven lumping," *Journal of Mathematical Biology*, vol. 62, no. 4, pp. 479–508, 2011.